Theoretical investigations of bond properties in graphite and graphitic silicon

YuChen Wang

Max Planck Institute of Microstructure Physics, Weinberg 2, D-06120 Halle, Germany
and Laboratory of Atomic Imaging of Solids, Chinese Academy of Sciences, Shenyang 110015, People's Republic China

Kurt Scheerschmidt* and Ulrich Gösele

Max Planck Institute of Microstructure Physics, Weinberg 2, D-06120 Halle, Germany
(Received 26 July 1999; revised manuscript received 18 October 1999)

Within the local-density approximation, the interlayer binding and the electronic properties of graphite and ''graphitic'' Si have been determined. For graphite, the optimized equilibrium lattice constant agrees well with the experimental value. The role of $2p_z$ orbitals (π states) turned out to be twofold: contributing a major part to the binding of C atoms within basal planes, and giving a minor contribution in the form of the overlay of $2p_z$ orbitals, which leads to weaker interlayer binding. The interlayer binding attributed to the interaction of C-C atoms in different layers yields the calculated binding energy as a function of the lattice constants and is applied to fit an additional Lennard-Jones-type empirical potential to be included in classical molecular-dynamics simulations. In contrast to that, the calculated energy pathways for ''graphitic'' Si show an extended region of minima within the range of $a = 3.84$ Å and for c varying from 5.50 to 6.68 Å having two lower levels, which indicates chemisorption and physical absorption. The obtained electronic density distribution demonstrates that the atoms in ''graphitic'' Si tend to form a structure with metal-like electron distributions. Nevertheless, a Lennard-Jones potential with restricted validity may be fitted to describe the weak long-range behavior, too.

I. INTRODUCTION

Graphite as a prototype layer material has been studied extensively due to its technological importance. Natural graphite exists in the forms of a hexagonal structure (Bernal structure)[1] and a rhombohedral structure.[2] Both forms of graphite consist of carbon atoms arranged in planar hexagonal networks. The stacking sequences of the carbon atom layers for hexagonal and rhombohedral structures are of $ABAB\ldots$ and $ABCABC\ldots$ types, respectively. The experimental results have shown that a given graphite sample usually contains 80% of the hexagonal structure, 14% of the rhombohedral structure, and 6% of disordered graphite,[2,3] and no rhombohedral structure has been detected in the isolated form without hexagonal components.

It is well known that graphite shows a difference in the binding character within and between the layers of carbon atoms. The spacing between the layers is larger than the C-C bond-length distance in the layers. The strong binding within the layers is described by the sp^2 ($2s$-$2p_x$-$2p_y$) hybridization of atomic orbitals (σ states), and the weak interlayer binding is derived from the nonhybridized $2p_z$ orbitals (π states) perpendicular to the graphitic planes. This results from the stacking of the graphene planes (three sp^2 hybrids forming a honeycomb structure) and the interlayer bindings due to p_z overlap as calculated, for instance, using the self-consistent-field pseudopotential local-density approximation (LDA).[4,5] The resulting band structure including bonding σ and π states and antibonding σ^* and π^* states shows valence and conduction bands, respectively. Theoretical studies of the electronic properties of hexagonal graphite[4–12] have demonstrated that normal to the basal planes a slight or no dispersion of the σ bands leads to a two-dimensional char-

acter of graphite although the π bands show some dispersion. The weak interactions between ''graphitic'' planes modify the ideal two-dimensional situation, which leads to a zero-gap semiconductor[13] and creates a semimetal. The interlayer interaction forces are commonly attributed to a van der Waals type of dynamics interaction between the electrons on adjacent sheets of carbon. However, within the LDA of the density-functional theory (DFT),[14–17] the contribution of the exchange correlation is of short-range type. Therefore, the interlayer binding would be poorly described by LDA if the interlayer binding in graphite is dominated by such short-range interactions. A previous calculation[11] using the LDA and the linearized augmented-plane-wave method really gives a poor result as to the interlayer cohesive energy and the interlayer distance compared with the experimental values. However, two LDA calculations[18,19] with accurate expressions for the kinetic-energy functional and carefully designed pseudopotentials and making use of a large number of plane waves recently showed that the obtained interlayer distances and cohesive energies may agree well with the experimental values. Thus it is confirmed that a careful LDA calculation can properly describe the interlayer binding in graphite, providing the proper balance between the attractive van der Waals interaction and other contributions to the cohesive energy. The obtained interlayer binding energies have been successfully fitted to the form of a Morse function, which agrees well with the experimental results, but failed to fit a function of the Lennard-Jones (LJ) type. In addition, at ambient pressure or at hydrostatic pressures of 5 and 10 GPa, the electronic structure of graphite has been calculated self-consistently using the method of full-potential linear-muffin-tin orbitals.[20]
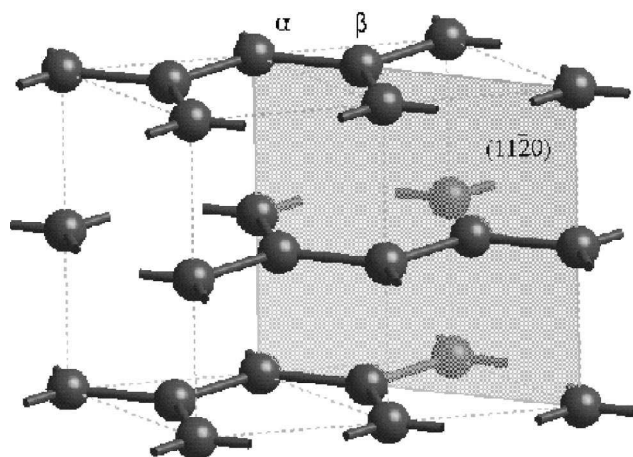
FIG. 1. Two unit cells of the $P6_3/mmc$ ''graphitic'' structures characterizing α and β type atoms and the (110) planes considered in the projections of electron densities.

As elements of group IV, both Si and C have the same valence electron number and a similar distribution of the outermost electrons for the free atoms. Therefore, to a certain extent, Si and C should have similar properties with respect to their chemistry and physics, as well as crystal structure. Carbon and silicon with diamond structure are among the materials most studied and best understood in science and technology. However, to our knowledge, there is no experimental report as to the existence of ''graphitic'' Si. From the theoretical point of view and based on the LDA with a pseudopotential, the ''graphitic'' Si has been investigated and regarded as a hypothetical material with a ratio of lattice constants c/a similar to that of graphite. The theoretical investigations lead to the conclusion that ''graphitic'' Si cannot exist due to its relatively weak binding, with a higher energy than those of the diamond phase. Thus the existence of ''graphitic'' Si would require a high negative pressure.[6] A recent theoretical investigation of the planarity of the aromatic stage of two-dimensional Si and Ge layers showed that Si and Ge prefer to form the corrugated aromatic stage.[21]

The present work is concerned at first with the interlayer bindings in graphite using total energy pseudopotential calculations. The investigation of the graphitic phase is limited to its hexagonal structure as the rhombohedral graphite occupies only a small part (15%) of natural graphite. The results of the calculations as to graphite show that the $2p_z$ orbitals (π states) contribute not only to the interlayer binding, but also to the C-C binding within the layers. The interlayer binding is attributed to the interaction between the C atoms in different basal planes. Using these properties a functionality of the LJ type is fitted. It is the basis for constructing a modified empirical potential, which reflects the short-range forces by a bond-order-type interaction and which shows a smooth transition to the present LJ fit. Details of this new potential will be reported in a forthcoming paper. To understand the similarities of and differences between C and Si, the hypothetical material, ''graphitic'' Si, is also investigated in terms of the interlayer binding and electronic structures. Although the calculations demonstrate the impossibility of a stable ''graphitic'' Si phase, the functionality proven between energy and lattice constant allows the fit of the long-range interaction of the LJ type.
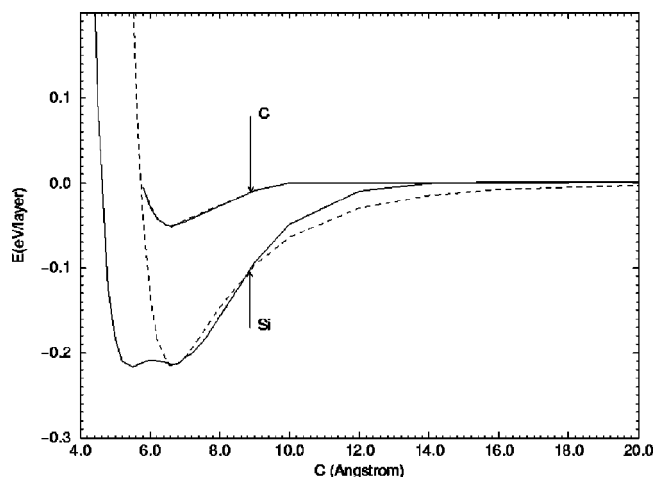

FIG. 2. The interaction minimum energy for graphite C and ''graphitic'' Si as function of the lattice parameter c for optimum a_0: DFT database simulated for the optimized lattice constant a_0 (C: 2.44 Å, Si: 3.86 Å) and c varying (continuous curves) and for best Lennard-Jones potential fit (dashed curves).

The paper is organized as follows: The method of the calculation is described briefly in Sec. II. The calculated results of graphite and ''graphitic'' Si are analyzed and discussed in Sec. III, including (1) the energy minimum pathways of interlayer binding, (2) electronic densities, and (3) fitting the calculated results to a Lennard-Jones function. Finally, the conclusions in Sec. IV discuss the applicability of the results to the refinement of empirical potentials.

II. METHOD OF CALCULATION

The calculations were performed using the pseudopotential method within the LDA. The optimized, norm-conserving, nonlocal pseudopotentials generated by the Q_c tuning method[22,23] were used in the Kleinman-Bylander form.[24] The *ab initio* calculations were carried out using the computer code CASTEP; the details are given elsewhere.[25] The crystallographic structures of the hexagonal ''graphitic'' phase belong to the $P6_3/mmc$ space group. The constructed
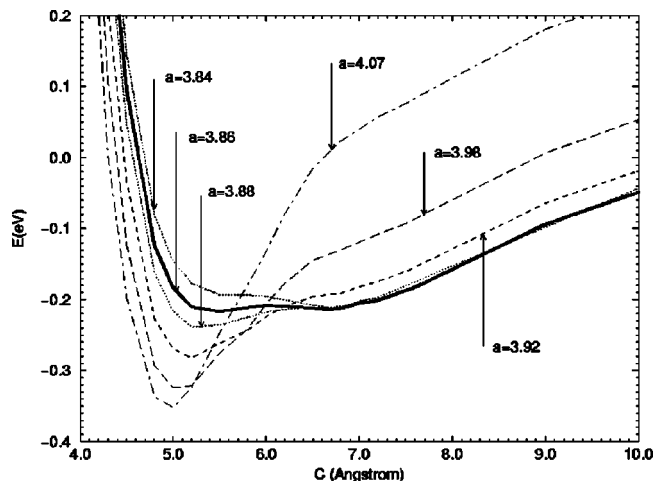

FIG. 3. Interaction energy minimum pathway for ''graphitic'' Si: The energy as a function of the lattice constant c using different lattice constants a as the parameter.

TABLE I. Comparison of the calculated lattice constants a, c, and interlayer binding energies E_{ib} for graphite and ''graphitic'' Si with experimental and other theoretical results. The values marked by * indicate that the a, c, and c/a were extracted from the minimum of physical absorption. The values in parentheses indicate that the calculations were performed with a fixed c/a ratio obtained from the experiment.

Source	Graphite				''Graphitic'' Si			
	a(Å)	c(Å)	c/a	E_{ib} (eV/layer)	a(Å)	c(Å)	c/a	E_{ib} (eV/layer)
Present	2.44	6.62	2.71	0.050	4.07	4.95	1.22	0.35
					3.86*	6.68*	1.73*	0.21*
Ref. 18	2.451	6.70	2.734	0.050				
Ref. 19	2.45	6.60	2.69	0.040				
Ref. 21	2.49				3.86			
Ref. 6	2.47	6.73	(2.726)		3.90	10.62	(2.726)	
Ref. 28 (Expt.)	2.461	6.709	2.726					
Ref. 29		5.60		0.22				
Ref. 30	2.47	6.74	2.725	0.12				
Ref. 31	2.45	6.87	2.802	0.06				
Ref. 32	2.450							
Ref. 11	2.459	6.828	2.773	0.28–0.16				
Ref. 33 (Expt.)				0.046				

primitive cell includes four atoms (two atoms for each ''graphitic'' plane and two planes per cell, see Fig. 1). The electronic wave functions are expanded in sets with a plane-wave basis up to an energy cutoff of 670 eV for C and 400 eV for Si. To understand the convergence of the calculated properties with respect to the number of k points, total-energy calculations for graphite with $a_0 = 2.44$ Å, $c_0 = 6.62$ Å, and for ''graphitic'' Si with $a_0 = 3.86$ Å and $c_0 = 6.68$ Å were performed using 14, 20, 40, and 56 symmetrized k points generated by the Monkhorst-Pack scheme.[26] The calculations using 56 k points were regarded to be completely accurate. The discrepancies of the calculated total energy for using 14, 20, and 40 points are 83, 3, and 3 meV for graphite, and 21, 2, and 2 meV for ''graphitic'' Si, respectively. That means that using 20 symmetrized k points, as done in the present paper, may provide sufficiently the desirable accuracy.

III. RESULTS AND DISCUSSION

A. Local energy minimum pathways of interlayer binding

In hexagonal ''graphitic'' structures, there are two kinds of nonidentical carbon (or silicon) atoms, denoted by α and β as sketched in Fig. 1. The α atoms have neighbors as counterparts immediately in adjacent layers, whereas β atoms are in juxtaposition. Thus the contribution of α atoms and β ones to the interlayer binding is different. The interlayer interaction energy within the area with one α and one β atom can be used to describe the interlayer binding. It can directly be obtained from the calculated total energies by $E_{ib} = (E_{struc} - E_\infty)/2$. Factor 2 indicates that each primitive cell contains two ''graphitic'' planes. Here, E_{struc} is the total energy of the primitive cell with different c and a values. E_∞ is the total energy obtained from the configuration with an optimized a value and large c values, whereas c/a must be chosen as large as to enable the interaction between the basal planes to be neglected. In the present work, the total energy changes by less than 0.03 meV/atom if the graphite lattice constant a is kept at the optimized value of 2.44 Å and the

lattice constant c is varied from 12.0 Å to 15.0 Å. For ''graphitic'' Si, the total energy change is less than 0.04 meV/atom if c is varied from 16.0 Å to 20.0 Å with a fixed at the optimized value of 3.86 Å. That means that the interaction energies between the layers may be neglected, if the values of the lattice constants c are larger than 12.0 Å for graphite and 16.0 Å for ''graphitic'' Si. Therefore it is reasonable to make use of the configurations with $a_\infty = 2.44$ Å and $c_\infty = 15.0$ Å, and $a_\infty = 3.86$ Å and $c_\infty = 20.0$ Å to calculate the E_∞ for graphite and ''graphitic'' Si, respectively.

The interaction energies as functions of the lattice constants c at fixed a_0, where the latter is always optimized beforehand, are used to illustrate the interlayer binding (cf. Fig. 2, solid lines only; the dashed curves are the finally fitted LJ potentials as discussed in Sec. III C below). The energy as a function of the lattice constant c shows a different behavior for graphite (C in Fig. 2) and ''graphitic'' Si (Si in Fig. 2). The optimum a_0 is chosen to be equal to the corresponding a_∞ as justified below. To evaluate the minimum configurations accurately, in the DFT calculations the lattice constant c was changed with a small step size of 0.01 Å around the energy minima. Very small discontinuities in the total energy curves arise at some points far from the minimum energy in graphite and far from the extended region of minima in ''graphitic'' Si. Though large cutoffs $E_{cut} = 700$ eV and 400 eV for C and Si, respectively, were used, the effect of numerical noise with the largest relative error estimated to be 10^{-4} cannot be cancelled, but should be minimized as analyzed in Ref. 19. Therefore, those discontinuous points have simply been crossed out.

For graphite, only one minimum occurs at $c_0 = 6.62$ Å (cf. the curve marked by C in Fig. 2), which does not change remarkably for varying a. The calculation of the interaction energy for different lattice constants a proves that the curve with a_0 is always the minimum energy pathway with respect to the parameter a and for varying c within the interval from 5.75 Å to 15.0 Å.
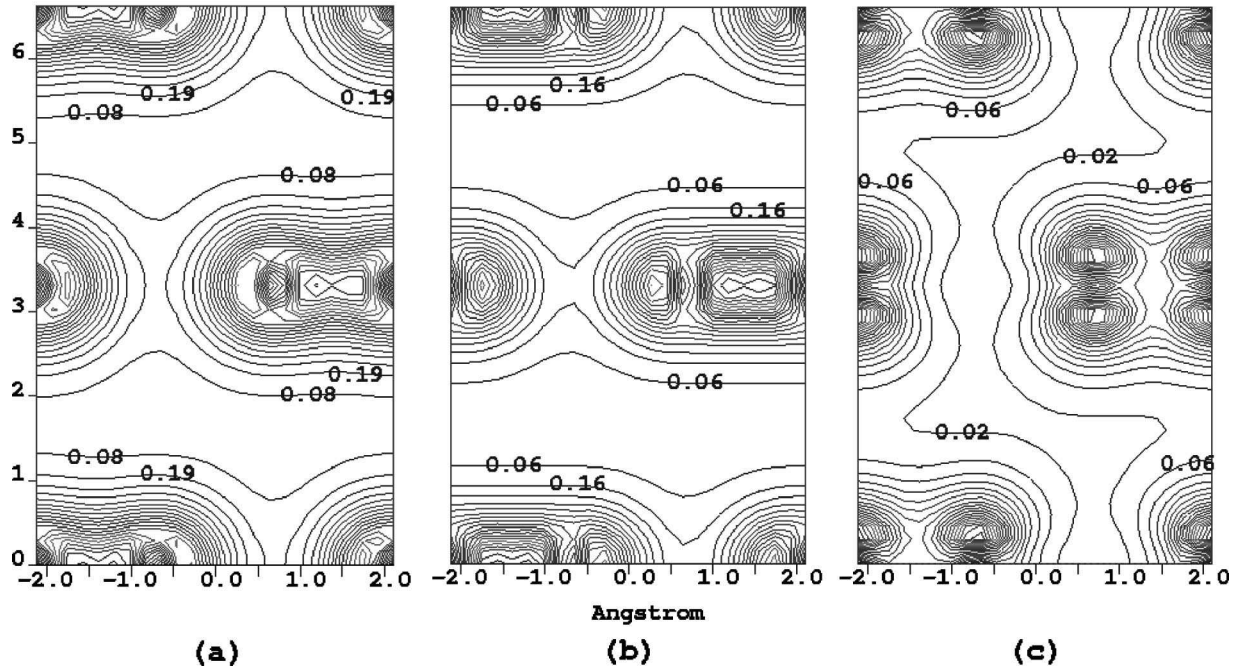
FIG. 4. Charge density distribution (eV/Å^3) within the (110) plane in graphite for (a) all electrons of occupied states, (b) all occupied σ states, and (c) all occupied π states ($a_0=2.44$ Å, $c_0=6.62$ Å).

In contrast to the results for graphite, in ''graphitic'' silicon (marked by Si in Fig. 2) an extended area of minima occurs from $c_0'=5.50$ Å to $c_0=6.68$ Å with $a_0=3.86$ Å being optimized. Though the energy only reveals a difference of 2 meV within this interval there are two flat minima, occurring at $c_0=6.68$ Å and $c_0'=5.50$ Å. This result is very different from that obtained by Yin and Cohen[6] who assumed that ''graphitic'' Si has the same value of $c/a=2.726$ as has graphite. To discuss the behavior of the energy minima, in Fig. 3 the minimum interaction energy pathway to optimize a is shown for ''graphitic'' Si. The pathway shows the energy minima as functions of the c variation with different lattice constants a used as parameters. In the case of graphite, as mentioned above, only one very stable minimum occurs; thus the respective curve need not be discussed. For $a \leqslant a_0=3.86$ Å, always an extended area of minima occurs having the deepest minimum at $c_0=6.68$ Å. However, with increasing lattice constants a the minimum at $c_0'=5.50$ Å in Fig. 2 becomes deeper and the band is broadened. For $a > a_0=3.86$ Å and with increasing a the overall energy increases and the minimum at $c_0=6.68$ Å disappears. The minimum at $c_0'=5.50$ Å in Fig. 2 becomes deeper and sharper. Furthermore, the calculations show that the absolute minimum occurs at $a=4.07$ Å and $c_0''=4.95$ Å with the lowest minimum energy of 107.34 eV/atom.

While the stable minimum in graphite at $c_0=6.62$ Å indicates that there is an energy barrier separating other interactions from that between the basal planes, the minima c_0, c_0', and c_0'' in Si are not well separated. The minimum at $c_0''=4.95$ Å reaches its absolutely deepest level for $a=4.07$ Å within the investigated configurations corresponding to the bond length in the diamond structure, which will be discussed below considering the electronic densities. Thus for the hypothetical ''graphitic'' Si the minimum pathways of the interlayer interaction energy can be described from c $=\infty$ to $c_{crit}=6.50$ Å by the curve with $a_0=3.86$ Å. As c becomes smaller than $c_{crit}=6.50$ Å the energy minimum pathway will follow the curve with the lowest energy as shown in Fig. 3. Therefore, those two minima shown by c_0 and c_0'' may be interpreted in terms of chemisorption at $c_0''=4.95$ Å and of physical absorption at $c_0=6.68$ Å. That no higher barrier occurs between the physical absorption and the chemisorption means that the ''graphitic'' structure with a large interlayer spacing in Si is meaningless. To verify this conclusion, using the same pseudopotential and 60 symmetrized k points, we also optimized Si configurations in the diamond structure. The obtained lowest energy is 107.94 eV/atom. Comparing the experimental difference of the cohesive energy of 0.025 eV/atom between the diamond and graphite (see the unpublished report of Brewer[27] for the cohesive energy at 0 K), the much higher energy difference of 0.60 eV/atom for Si indicates that the ''graphitic'' structure is meaningless, too. The critical value c_{crit} may be used to separate short and long-range interactions as well as to limit the validity of the potential fit before structural changes occur.

The experimental values of the lattice constants a_0 and c_0 for graphite[6] were measured to be 2.461 Å and 6.709 Å, respectively. In the present work, the theoretical equilibrium lattice constants a_0 and c_0 for graphite were determined directly from the configuration with the lowest energy. Considering for ''graphitic'' Si the energy pathway with $a_0=3.86$ Å, which is the curve with the overall lowest energy fulfilling the restrictions of stability discussed above, the lattice constants $a_0=3.86$ Å and $c_0=6.68$ Å were extracted from the physical absorption minimum as given in Fig. 2. All attained equilibrium lattice constants together with the experimental and other theoretical values are listed in Table I. Especially for graphite, there is a good agreement with the calculated values $a_0=2.44$ Å and $c_0=6.62$ Å.
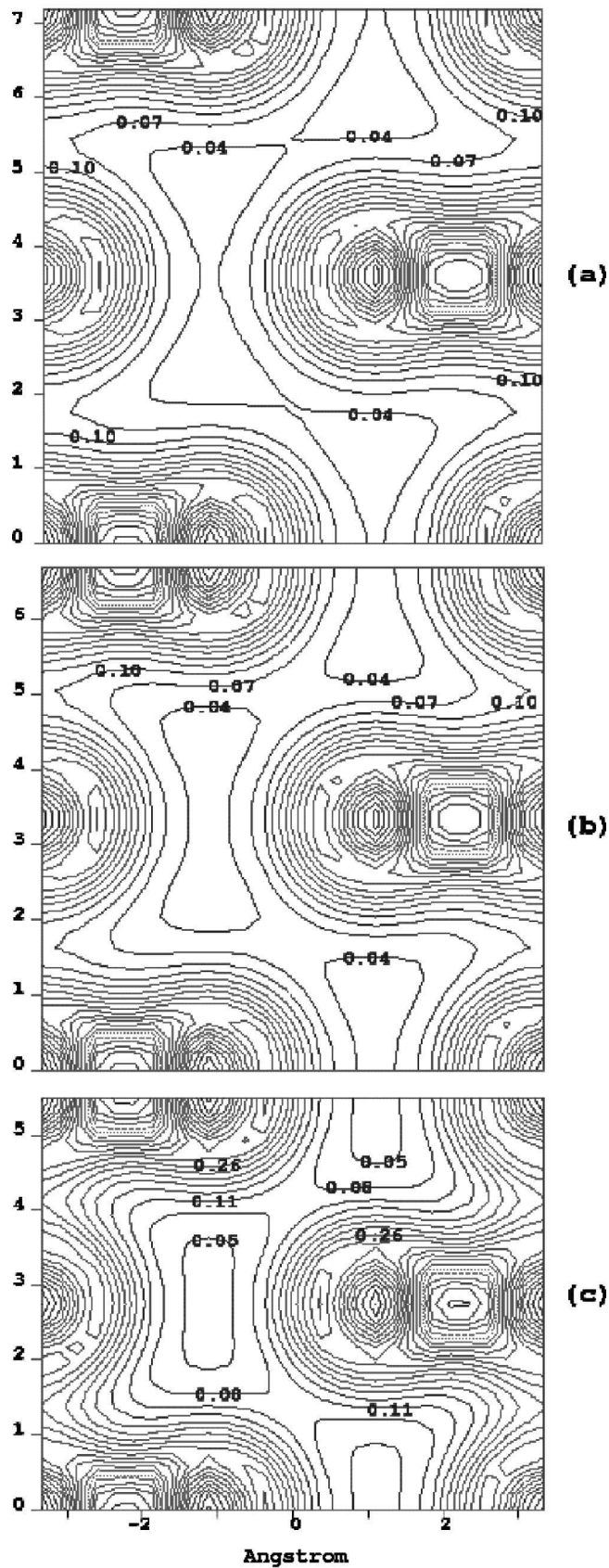
FIG. 5. Electronic density distribution (eV/Å^3) within the (110) plane in ''graphitic'' Si for $a=3.86$ Å and $c=7.2$ Å (a), 6.68 Å (b), and 5.5 Å (c).

The interlayer binding energies E_{ib}, obtained from the calculated lowest energy by $E_{ib}=(E_{low}-E_\infty)/2$, are also listed in Table I. The interlayer binding energy of 0.05 eV/layer for graphite agrees well with the experimental and theoretical values in Refs. 19 and 21. This indicates that our result reasonably well reflects the weak interlayer interaction of the van der Waals type in graphite, too. For ''graphitic'' Si and using the energy value at $a_0=3.86$ Å and $c_0=6.68$ Å the interlayer binding energy of 0.21 eV/layer is obtained. Though stronger than that in graphite, the binding energy still indicates that the interlayer interaction is a weak one. The binding energy of 0.35 eV/layer at $a_0=3.86$ Å and $c_0''=4.95$ Å indicates that the interlayer interaction at the minimum of chemisorption is stronger than that at the minimum of physical absorption. A detailed discussion will be given in Sec. III B considering the electronic density distribution as a function of the lattice parameters.

B. Electronic densities

Figure 4 shows resulting electronic structures of the lowest energy configuration within the (110) planes of graphite. In Fig. 4(a) the character of stronger covalent bonds between the C-C atoms within the basal planes and weaker interactions between the C atoms in different basal planes is manifested evidently. The lower electronic density of the order of 0.08 eV/Å^3, occurring in the region between the basal planes, indicates that the interaction between the interplane C atoms is weak. In order to understand the binding features of the $2p_z$ orbitals of C atoms within the basal plane and between the basal planes, the electronic densities of all σ states and of all π states have been used [cf. Figs. 4(b) and 4(c), respectively] to illustrate their contributions to the binding. The electron density distributions of all σ states shown in Fig. 4(b) really present features of the sp^2 hybridized 2s, $2p_x$, and $2p_y$ atomic orbitals within the basal planes. However, the role of all π-state electrons shown in Fig. 4(c) is twofold: (i) providing a π-bond binding between all C atoms within the basal plane, which is added to the original σ bonds, strongly correlating to the C atoms, and (ii) contributing to the interlayer binding due to a superposition of the orginal $2p_z$ orbitals. The lower density of the order of 0.02 eV/Å^3, present in the region between the basal planes as shown in Fig. 4(c), indicates that the interplane C-C binding of different layers is weaker than the in-plane binding. This explains why the interlayer binding is a weak interaction in graphite.

The distribution of electronic densitiy of ''graphitic'' Si within the (110) planes is shown in Fig. 5, with $a_0=3.86$ Å and $c=7.2$ Å, 6.68 Å, and 5.5 Å in Figs. 5(a), 5(b), and 5(c), respectively. In Figs. 5(a) and 5(b) the electronic density between the interplane Si atoms is lower than that within the basal planes, indicating that the binding of interplane Si-Si atoms is weaker than that within the basal planes. The lower density of the order of 0.07 eV/Å^3 and 0.10 eV/Å^3, occurring in the regions between the basal planes, is very similar to that of C in Fig. 4(a). It indicates that the interlayer interaction is weak, too. Nevertheless, the density increases with c decreasing from 7.20 Å to $c_0=6.68$ Å. This explains why the minimum at $c_0=6.68$ Å may be regarded as the optimum value of the weak interlayer interactions, i.e., the minimum of the physical absorption.

The electronic density of the order of 0.26 eV/Å^3 occurring in Fig. 4(c) indicates that the chemical bond is formed between the interplane Si atoms and the interlayer interaction is not a weak one. The binding between the in-plane Si atoms in ''graphitic'' Si becomes weaker, whereas the interlayer binding becomes stronger. In all calculated density patterns of Fig. 5 and in contrast to Fig. 4, we cannot clearly display the distribution of electron states, because the occupied orbitals in the ''graphitic'' phase cannot be distinguished. However, from the obtained lowest-energy configuration at $a = 4.07$ Å and $c_0'' = 4.95$ Å, we may find that the interlayer distance $c_0''/2 = 2.475$ Å is close to the in-plane bond length of 2.35 Å. For this configuration, the valence electron distribution of Si atoms does not only contribute to the in-plane Si-Si bonds, but also to the interplane Si-Si bonds. Considering that the neighbor number of each Si atom exceeds four and that the order of the electronic density between interplane Si atoms becomes close to that between in-plane Si atoms, one can conclude that the distribution of the electrons of the Si atoms in a ''graphitic'' structure will tend to give a metal-like electron distribution.

C. Fitting the calculated results to a Lennard-Jones function

As dissussed above, the obtained interlayer binding energy for graphite (50.0 meV/layer) is in good agreement with the experimental value (46 meV/layer) and theoretical ones[18,19] (cf. Table I). In Ref. 19, the obtained interlayer interaction energies were successfully fitted to the form of a Morse function without considering the difference between the α and β atoms. Here, the interlayer binding is attributed to the interaction between the C atoms in different basal planes, which is regarded to be of the van der Waals type and may be described by the LJ function $E_{c-c} = 4\epsilon[(\sigma/R_{ij})^{12} - (\sigma/R_{ij})^6]$. Then, within the range of the basal plane (including one α atom and one β atom), the interlayer binding energy E_{ib} (in the unit of eV/layer) is fitted to the function $E_{ib} = \Sigma_{i=a,b}\Sigma_{j=1,7}4\epsilon[(\sigma/R_{ij})^{12} - (\sigma/R_{ij})^6]$. Here, R_{ij} indicates the distance between the ith C atom in the reference basal plane and the jth C atom in the nearest-neighbor basal plane, where a maximum of seven nearest-neighbor atoms within the adjacent planes is assumed. The method of simulated annealing was used to fit the theoretical values to the LJ function. The optimized parameters ϵ and σ are 0.001 88 eV and 3.3264 Å, respectively. Figure 2 (dashed curves) shows the comparison between the calculated data points and the fitted LJ potential; they agree fairly well. The fitted LJ form can also be used to handle the long-range interaction of C atoms within the validity of the sp^2 hybridization.

For ''graphitic'' Si, the situation is very different from that in graphite due to the existence of at least two local minima. However, based on the analysis of the energy path-

way and the electronic densities, the obtained data for all $c > c_{crit} = 6.50$ Å with $a_0 = 3.86$ Å as shown in Fig. 2 describe the long-range behavior and are used in the simulated annealing procedure to fit the weak long-range potential. Applying the restricted fit procedure one gets a well-fitted LJ potential with $\epsilon = 0.0171$ eV and $\sigma = 3.3362$ Å for extending the empirical potential to the long-range region, too.

IV. CONCLUSIONS

Based on the interlayer interaction minimum energy levels and the electronic structures obtained from total-energy pseudopotential calculations, the most important results can be summarized as follows.

(1) In graphite, the role of the $2p_z$ orbitals (π states) of the C atoms is twofold: First, the $2p_z$ orbitals make a contribution to the in-plane C-atom binding, providing a stronger C-atom binding than does the combination with contributions of the sp^2 hybridization (σ states). Second, there is an additional contribution to the interlayer binding in the form of an overlap of $2p_z$ orbitals. The interlayer binding is attributed to the interaction of interplane C atoms, and is fitted to the form of a LJ function. The good agreement between the theoretical results and the experimental data demonstrates that a LJ potential function can describe the interlayer interaction appropriately well.

(2) Compared to graphite, the binding between the in-plane Si atoms in ''graphitic'' Si becomes weaker, whereas the interlayer binding becomes stronger. The interlayer interaction is no longer of the van der Waals type due to chemical bonds formed between the in-plane Si atoms. The resulting metal-like electron distribution means that it is impossible for Si to exist in the ''graphitic'' phase. Nevertheless, a restricted LJ potential fit enables one to describe long-range interactions, too.

For including the interlayer forces into empirical potentials it is necessary to parametrize a suitably chosen short-range potential and to smoothly combine both the short-range and the LJ potentials at a common cutoff value. Different empirical potentials are tested and fitted, and a new short-range parametrization has been found. Respective details, the comparison with bond-orderlike analytical developments,[34] and the test of applicability especially for interacting surfaces as, e.g., relevant for wafer bonding,[35] will be published in a forthcoming paper.

---

*Author to whom all correspondence should be addressed. FAX: +49-0345-5582917. Electronic address: schee@mpi-halle.de, http:\\www.mpi-halle.de

[1] J.D. Bernal, Proc. R. Soc. London, Ser. A **160**, 749 (1924).

[2] H. Lipson and A.R. Stockes, Proc. R. Soc. London, Ser. A **181**, 101 (1942).

[3] R.R. Haering, Can. J. Phys. **36**, 352 (1958).

[4] J.C. Boettger, Phys. Rev. B **55**, 11 202 (1997).

[5] Ç. Kiliç, H. Mehrez, and S. Ciriaci, Phys. Rev. B **58**, 7872 (1998).

[6] M.T. Yin and M.L. Cohen, Phys. Rev. B **29**, 6996 (1984).

[7] J.-C. Charlier, X. Gonze, and J.-P. Michenaud, Phys. Rev. B **43**, 4579 (1991).

[8] R.C. Tatar and S. Rabii, Phys. Rev. B **25**, 4126 (1982).

[9] N.A. Holzwarth, S.G. Louie, and S. Rabii, Phys. Rev. B **26**, 5382 (1982).

[10] M. Posternak, A. Baldereschi, A. Freeman, E. Wimmer, and M. Weinert, Phys. Rev. Lett. **50**, 761 (1983).

[11] H.J.F. Jansen and A.J. Freeman, Phys. Rev. B **35**, 8207 (1987).

[12] D. Tomanck, R.M. Wentzcovitch, S.G. Louie, and M.L. Cohen, Phys. Rev. B **37**, 3134 (1988).

[13] P.R. Wallace, Phys. Rev. **71**, 622 (1947).

[14] P. Hohenberg and W. Kohn, Phys. Rev. **136**, B864 (1964).

[15] W. Kohn and L.J. Sham, Phys. Rev. **140**, A1133 (1965).

[16] J.P. Perdew and A. Zunger, Phys. Rev. B **23**, 5048 (1981).

[17] D.M. Ceperley and B.J. Alder, Phys. Rev. Lett. **45**, 566 (1980).

[18] M.C. Schabel and J.L. Martins, Phys. Rev. B **46**, 7185 (1992).

[19] J.-C. Charlier, X. Gonze, and J.-P. Michenaud, Europhys. Lett. **28**, 404 (1994).

[20] R. Ahuja, S. Auluck, J. Trygg, J.M. Wills, O. Eriksson, and B. Johansson, Phys. Rev. B **51**, 4813 (1995).

[21] K. Takeda and K. Shiraishi, Phys. Rev. B **50**, 14 916 (1994).

[22] J.S. Lin, A. Qteish, M.C. Payne, and V. Heine, Phys. Rev. B **47**, 4174 (1993).

[23] M.H. Lee, Ph.D. thesis, University of Cambridge, United Kingdom, 1995.

[24] L. Kleinman and D.M. Bylander, Phys. Rev. Lett. **48**, 1425 (1982).

[25] M.C. Payne, M.P. Teter, D.C. Allan, T.A. Arias, and J.D. Joannopolous, Rev. Mod. Phys. **64**, 1045 (1992).

[26] H.J. Monkhorst and J.D. Pack, Phys. Rev. B **13**, 5188 (1976).

[27] L. Brewer, Lawrence Berkeley Laboratory Report No. LBL-37220 (unpublished).

[28] J. Donohue, *The Structures of the Elements* (Krieger, Malabar, Florida, 1982), p. 256.

[29] D.P. Divincenzo, E.J. Mele, and N.A.W. Holzwarth, Phys. Rev. B **27**, 2458 (1983).

[30] R.H. Baughman, H. Eckhardt, and M. Kertesz, J. Chem. Phys. **87**, 6687 (1987).

[31] S.B. Trickey, F. Müller-Plathe, G.H.F. Diercken, and J.C. Boettger, Phys. Rev. B **45**, 4460 (1992).

[32] M. Weinert, E. Wimmer, and A.J. Freeman, Phys. Rev. B **26**, 4571 (1982).

[33] L.A. Girifalco and R.A. Lad, J. Chem. Phys. **25**, 693 (1956).

[34] D. Conrad and K. Scheerschmidt, Phys. Rev. B **58**, 4538 (1998).

[35] A. Plössl and G. Kräuter, Mater. Sci. Eng., R. **25**, 1 (1999).